

Elastic Electron Scattering Experiments with  $N^{15}$ \*

E. B. DALLY†

*High Energy Physics Laboratory, Stanford University, Stanford, California 94305*

AND

M. G. CROISSIAUX

*High Energy Physics Laboratory, Stanford University, Stanford, California 94305 and  
Institut de Recherches Nucleaires, Strasbourg, France*

AND

B. SCHWEITZ

*Institut de Recherches Nucleaires, Strasbourg, France*

(Received 15 August 1969)

The nucleus of  $N^{15}$  has been investigated by the electron scattering technique at incident energies of 250 and 400 MeV. The first diffraction minimum has been observed and measured. The data have been analyzed by using two nuclear charge density distributions: the Fermi model and the shell model. A phase-shift program was used for the analysis. A value for the radius and skin thickness of the  $N^{15}$  nucleus is given, although the data do not fit the diffraction minimum. For the Fermi model, the rms radius is 2.7 F; the shell model yields 2.6 F.

**M**ANY light nuclei have been investigated by the electron scattering technique. In this report we would like to present the results of elastic electron scattering experiments that have been performed on  $N^{15}$ .

The isotope  $N^{15}$  has a spin  $\frac{1}{2}$ , a magnetic moment equal to  $-0.283$  nuclear magnetons, and no quadrupole moment. Its natural isotopic abundance is 0.37%. The abundant nitrogen isotope  $N^{14}$  is odd-odd, and the addition of the neutron closes a shell, leaving a proton hole. Thus, among the light nuclei,  $N^{15}$  should be an interesting nucleus to study.<sup>1</sup>

## EXPERIMENTAL METHOD

The electron scattering technique has been frequently presented in the literature. The experimental installation at Stanford Mark III linear accelerator has been discussed in detail in numerous articles.<sup>2</sup>

The electron beam from the accelerator enters a beam switchyard where the energy and energy spread are defined. The energy spread of the beam was set to 0.25%. We have recalibrated the deflecting magnet of this system using the floating wire technique. The measurements were monitored with a nuclear magnetic resonance (NMR) probe, whose response was tied to the floating wire calibration. During the experiment, the beam energy was set and monitored by the NMR system. An error of  $\pm 0.2\%$  has been assigned to this energy calibration.

The beam was focused and aimed properly by viewing the beam spot on a zinc sulphide screen. The position was frequently checked during data runs. After passing through the target, the beam was stopped in a large Faraday cup. A precision current integrator was used to measure the charge.

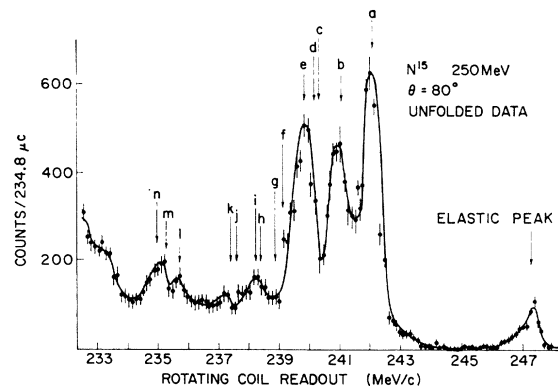


FIG. 1. Typical spectrum from  $N^{15}$  collected from the 100-channel ladder apparatus. The letters indicate the known position of excited levels. The first letter *a* refers to the doublet at 5.27 and 5.30 MeV (unresolved by the apparatus).

The  $N^{15}$  used as a target in this experiment was in the form of liquid heavy ammonia ( $N^{15}H_3$ ). The conversion of  $N^{15}$  to heavy ammonia, and the construction of the target, have been described in a recent article.<sup>3</sup> The target material was analysed in a mass spectrometer to look for the presence of  $N^{14}$ . Such tests showed the isotopic content to be 99.7%  $N^{15}$  and 0.3%  $N^{14}$ . The target cell presented to the beam was a rectangle 40 mm by 20 mm. Stainless steel, 12  $\mu$  thick, was used as window material. The target thickness was approximately 7.5 mm. This thickness was not very well known

\* Work supported in part by the U.S. Office of Naval Research under Contract No. Nonr 225 (67).

† Present address: Stanford Linear Accelerator Center, Stanford, Calif.

<sup>1</sup> A preliminary experiment was undertaken at the Accélérateur Linéaire Orsay (France) by E. Dally, M. Croissiaux, L. Paul, and T. Stovall (unpublished) at an energy of 180 MeV. The results are consistent, although known less precisely than the results of the present experiment.

<sup>2</sup> See, e. g., F. A. Bumiller, M. Croissiaux, E. Dally, and R. Hofstadter, Phys. Rev. **124**, 1623 (1961).

<sup>3</sup> E. B. Dally and M. Croissiaux, Rev. Sci. Instr. **38**, 646 (1967).

because of the variable bulge of the stainless-steel window used to contain the liquid heavy ammonia. The collision energy loss in the target, for both the 250- and 400-MeV data, was close to 0.5 MeV. The energy spread introduced by the Landau straggling was about 0.1%, which is less than the energy spread of the incident beam.

In order to measure the background, empty target runs were necessary. Such measurements were made using a dummy target cell whose windows were cut from the same material as those of the target. The target assembly was mounted in a large vacuum-tight scattering chamber. This assembly was suspended from a large cover plate, which completed the vacuum enclosure. The target cell was mounted on a small circular plate that could be rotated and whose center was eccentric to the scattering center. In this way, the target was easily removed from the beam line for background measurements. The empty target was mounted on the regular target ladder system of the scattering chamber and was run into the beam line when needed. The angle to the beam line of both target and empty target was also variable.

Electrons scattered from the target were analyzed in momentum by the Stanford 72-in. double-focusing spectrometer. This spectrometer was rotated to the desired angle by a carriage system. Variable horizontal and

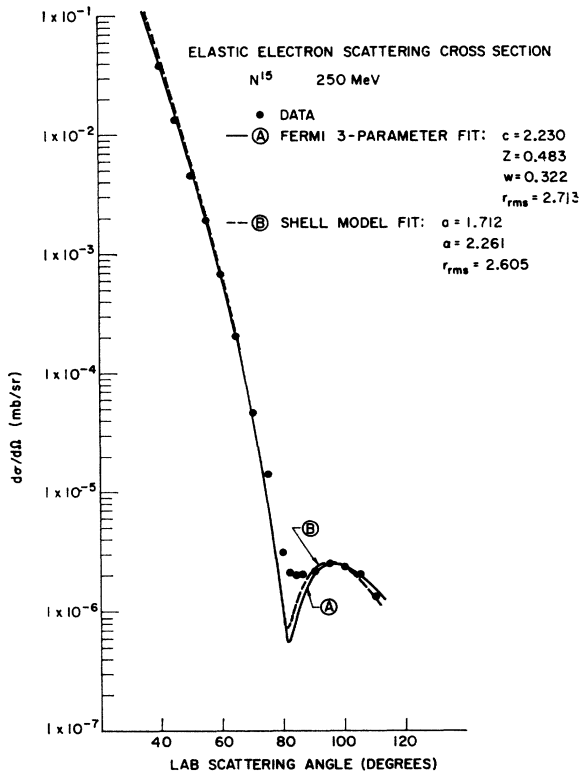


FIG. 2. Elastic electron scattering cross section versus laboratory angle for  $N^{15}$ . Incident energy is 250 MeV. The curves are calculated by a phase-shift program as described in the text.

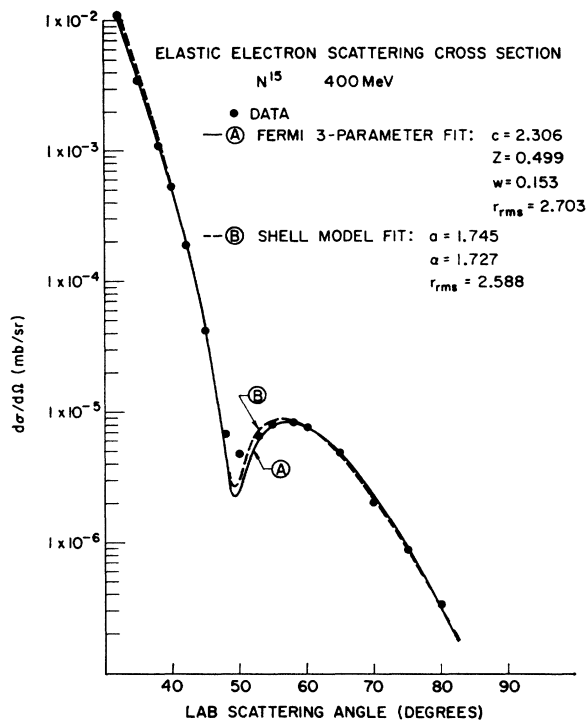


FIG. 3. Same as Fig. 2. Incident energy is 400 MeV.

vertical entrance slits defined the solid angle. The total angular spread of the slits subtended an angle of  $1.8^\circ$ . The field of the spectrometer was adjusted to a given value and monitored by a sensitive rotating coil system.<sup>4</sup> The exact location of scattering peaks could be reproduced on different nights by appropriately setting the magnetic field of the beam switchyard and 72-in. spectrometer with the use of the NMR and rotating coil systems, respectively.

The scattered electrons that passed through the vacuum chamber of the spectrometer were focused according to their momentum along a focal plane at the exit of the spectrometer. This focal plane contained 100 scintillation counters, each counter subtending an average momentum bite of 0.08%. The output of liquid Čerenkov backing counters was placed in coincidence to form a counter telescope. This 100-channel "ladder" with its associated electronic circuitry formed a data accumulation system.<sup>5</sup> Between beam pulses, the counts recorded during a beam pulse were read into a memory used for accumulation and continuous display. At the end of each data run, the accumulated information was dumped onto magnetic tape via the core of an IBM 7700 computer.

<sup>4</sup> F. A. Bumiller, J. F. Oeser, and E. B. Dally, in *Proceedings of an International Conference on Instrumentation for High-Energy Physics* (Wiley-Interscience, Inc., New York, 1960).

<sup>5</sup> L. R. Suelzle, thesis, Stanford University, 1966 (unpublished); and L. R. Suelzle and M. R. Yearian, in *Proceedings of the International Conference on Nucleon Structure at Stanford University, 1963*, edited by R. Hofstadter and L. Schiff (Stanford University Press, Stanford Calif., 1964), p. 360.

TABLE I. Measured electron scattering cross sections and errors for  $N^{15}$  at 250 MeV.

Scattering angle (deg)	Cross section ( $10^{-33}$ cm <sup>2</sup> /sr)	Errors ( $10^{-33}$ cm <sup>2</sup> /sr)
40	37 700	$\pm 2400$
45	13 600	800
50	4 650	300
55	1 960	118
60	691	44
65	210	13
70	47.7	2.9
75 <sup>a</sup>	14.2	0.85
80 <sup>a</sup>	3.10	0.19
82 <sup>a</sup>	2.12	0.13
84 <sup>a</sup>	2.07	0.15
86 <sup>a</sup>	2.06	0.13
90	2.15	0.17
95	2.57	0.15
100	2.40	0.14
105	2.08	0.12
110	1.37	0.10

<sup>a</sup> These data points not used for the phase-shift analysis (see text).

Data were collected in the following sequence: At the beginning of each run, the relative efficiencies of the 100 channels had to be determined. This was done by taking from six to ten carbon spectra, the central momentum of successive spectra being displaced about 5 MeV. Such spectra were collected in the region where the spectrum was more or less smooth, with no prominent structure. This procedure has been described by Crannell and Suelzle.<sup>6</sup> At a given incident energy and angle, a  $N^{15}$  spectrum was accumulated. For each full target spectrum, an empty target spectrum was taken. In addition, at each point an electron-proton scattering peak was measured from the hydrogen in the  $N^{15}H_3$ . With the use of the well-known electron-proton scattering cross sections, the proton scattering peaks provided the normalization to calculate the absolute  $N^{15}$  cross sections. A  $N^{15}$  spectrum is shown in Fig. 1. One can see not only the elastic peak, but also peaks corresponding to several excited levels. The analysis for the first levels (whose excitation is less than 8 MeV) is underway and will be published.

#### DATA REDUCTION

A first step in the data reduction was done off-line at the Stanford Computation Center.<sup>7</sup> In this data reduction program, there were several options available. One option provides for an automatic radiative correction to be applied to the data. This was done to the elastic scattering and excited levels of the spectrum shown in

<sup>6</sup> H. L. Crannell and L. R. Suelzle, Nucl. Instr. Methods **44**, 133 (1966).

<sup>7</sup> This program was written by H. L. Crannell (private communication).

Fig. 1. For the elastic scattering data, a counting rate correction was applied. During the data accumulation, the maximum counting rate allowed in the peak channel gave approximately a 4% correction. Since the Mark III beam is very steady on a pulse-to-pulse basis, these small corrections are accurate. An internal clock recorded the time during a data run and this time was recorded on the data tape. The program corrected the data, channel by channel, for the counting rate losses, with the use of this time. The computer calculated the channel efficiencies from the carbon spectra and corrected the data, channel by channel, with the appropriate efficiency factor. These factors were typically of the order of a few percent correction. The statistical error of the efficiency correction was folded into the statistical errors of the data, which had been carried through all parts of the data reduction. Finally, background runs were normalized to the same conditions of integrated beam and slit opening as for the full target data, and a channel-by-channel background subtraction was made. The data were presented in tabular and plotted form with their errors.

Corrections were made for the radiative losses to the proton elastic peak.<sup>8</sup> Such corrections were not made by the computer. A cut was made in the tail of the proton peak. The radiative corrections, necessary to account for the electrons lost below this cut, consisted of two parts: The electrons that underwent a bremsstrahlung process in the target and lost sufficient energy to fall beyond the cut, and those that emitted photons

TABLE II. Measured electron scattering cross sections and errors for  $N^{15}$  at 400 MeV.

Scattering angle (deg)	Cross section ( $10^{-33}$ cm <sup>2</sup> /sr)	Errors ( $10^{-33}$ cm <sup>2</sup> /sr)
32	11 260	$\pm 510$
35	3 540	150
38	1 127	45
40	536	21
42	189	87
45	41.8	15
48 <sup>a</sup>	6.88	0.40
50 <sup>a</sup>	4.87	0.20
53 <sup>a</sup>	6.51	0.38
55	8.19	0.27
58	8.12	0.29
60	7.70	0.22
65	4.91	0.14
70	2.05	0.082
75	0.890	0.046
80	0.340	0.015

<sup>a</sup> These data points not used for the phase-shift analysis (see text).

<sup>8</sup> N. Meister and D. Yennie, Phys. Rev. **130**, 1210 (1963); and H. R. Bethe and J. Ashkin, in *Experimental Nuclear Physics*, edited by E. Segré (Wiley-Interscience, Inc., New York, 1953), Vol. I, p. 272.

of sufficient energy via the Schwinger process. In the full target runs, the electrons (incident and scattered) lost an energy corresponding, on the average, to a target with the thickness of the liquid ammonia (corrected for target angle). In the empty target runs, there was no energy loss due to the target. The net result is that the elastic peak of N<sup>15</sup> for full target is slightly shifted toward the low-energy side, relative to the empty target peak (material of the stainless-steel foils). To compensate for this effect when taking empty target data, the incident energy was reduced by an amount equal to the average energy loss of the full target condition. Another small correction arises from Landau straggling, that is, from electrons whose energy losses in the target from ionization were large enough so that they appeared in the spectrum below the cut. Because the proton elastic peak rises out of the radiative tail of the continuum of the N<sup>15</sup> scattering, there was some arbitrariness in determining the base line for these normalizing peaks.

The absolute cross sections were calculated first by normalizing the N<sup>15</sup> to the proton scattering, as previously mentioned, and secondly, for a check, by taking a measured value for the target thickness and calculating them directly, using the measured integrated charge, and the known solid angle. Actually these two results were the same within a few percent and the values tracked one another, the normalized results being consistently slightly lower in value. We have presented the normalized cross sections as the best absolute values because of the uncertainty of the target thickness.

#### ANALYSIS OF THE DATA

The angular distributions of N<sup>15</sup> at 250 and 400 MeV are presented in Figs. 2 and 3, and the cross sections with errors are given in Tables I and II. The errors shown in Tables I and II are the combined statistical and estimated systematic errors. The 400-MeV data have typically 3-4% errors, whereas, the 250-MeV data have 5-6% errors. Some of the large-angle data have larger errors because of poorer statistical accuracy.

An attempt has been made to fit the data to two different charge density distributions. Such fits were made with the use of phase-shift calculations. The computer routine that we used was written by Heisenberg,<sup>9</sup> and is based on the original work of Yennie,

TABLE III. Fermi three-parameter fit.

Energy	$c$ (F)	$z$ (F)	$w$	rms radius (F)	$\chi^2$	Degrees of freedom
250	2.230	0.483	0.322	2.713	8.7	9
400	2.316	0.500	0.138	2.703	15.5	10

<sup>9</sup> J. Heisenberg (private communication).

TABLE IV. Shell-model fit.

Energy	$\alpha$	$a$ (F)	rms radius (F)	$\chi^2$	Degrees of freedom
250	2.261	1.712	2.605	20.8	10
400	1.723	1.746	2.588	27.7	11

Ravenhall, and Wilson.<sup>10</sup> The performance of this routine has been compared with the results of another widely used phase-shift code.<sup>11</sup> It has been tested on several nuclei over a large range of atomic numbers and has been found to give the same results. The angular resolution of the spectrometer is folded into the fitted cross sections.

The charge distributions that were used are the Fermi three-parameter distribution and a shell-model distribution. The Fermi distribution is given by

$$\rho(r) = (1 + wr^2) / (1 + e^{(r-c)/z}), \quad (1)$$

where  $c$  is approximately the radius at the one-half density point,  $z$  is the thickness parameter, which is related to  $t$ , the thickness of the charge density distribution from the 10 to 90% density points in the fall-off region  $t$  is given approximately by  $t = 4.4z$ .  $w$  has the effect of introducing a bulge or a dip in the central region of the charge distribution. The Fermi distribution has been used to fit nuclei over the entire periodic table, and an extensive amount of data and parameters have been accumulated. These results have been summarized recently by Collard and Hofstadter.<sup>12</sup>

The shell-model calculation was made with the use of

$$\rho(r) = [1 + (\alpha/a^2)r^2] \exp(-r^2/a^2). \quad (2)$$

When this is corrected for the finite proton size and nuclear recoil, the folded distribution becomes

$$\rho(r) = \{1 + \frac{3}{2}\alpha[1 - (a^2/a_m^2)] + (\alpha a^2 r^2/a_m^4)\} \times \exp(-r^2/a_m^2), \quad (3)$$

where  $a_m^2 = [(A-1)/A]a^2 + \frac{2}{3}a_p^2$ .  $\alpha$  and  $a$  are the shell-model parameters. In the shell-model description,  $\alpha$  is normally related to the level spacing and is theoretically given by  $\alpha = \frac{1}{3}(Z-2)$ . ( $Z$  equals nuclear charge.) Here we have treated  $\alpha$  as a free parameter to be adjusted to yield the best fit.  $a_p$  is related to the proton radius;  $a_p^2 = \frac{2}{3}\langle r_p^2 \rangle$ .  $A$  is the atomic number.

The phase-shift calculations have given fits that are satisfactory in the regions away from the diffraction minimum. However, at the diffraction minimum there

<sup>10</sup> D. R. Yennie, D. Ravenhall, and R. N. Wilson, *Phys. Rev.* **95**, 500 (1954).

<sup>11</sup> See, e.g., J. B. Bellicard, P. Bounin, R. E. Frosch, R. Hofstadter, J. B. McCarthy, F. J. Urbane, M. R. Yearian, B. C. Clark, R. Herman, and D. G. Ravenhall, *Phys. Rev. Letters* **19**, 527 (1964).

<sup>12</sup> H. Collard and R. Hofstadter, *Physikalisches-Chemisches Tabellen Landolt-Bornstein* (Springer-Verlag, Berlin, 1967 New Series, Group I, Vol. 2, p. 21).

TABLE V. Fermi two-parameter fit.

Energy	$c$ (F)	$z$ (F)	rms radius (F)	$\chi^2$	Degrees of freedom
250	2.476	0.498	2.666	12.1	10
400	2.429	0.504	2.654	34.5	11

is always a large difference between the fit and the data for both 250- and 400-MeV data. The fitted minima are deeper and narrower than the data points. In order to avoid a distortion of the values of the fitted parameters, which would be caused by such large differences, we have excluded from the analysis those data points in the region of the diffraction minima. The curves in Figs. 2 and 3 show the fits made without these data points. The summary of the parameters found through the phase-shift calculations are shown in Tables III and IV for the Fermi and shell models, respectively. Calculations made with the Fermi two-parameter formulation ( $w=0$ ) are shown in Table V. Two parameters are sufficient to fit the data at 250 MeV, but not at 400 MeV, as expected. The radius is somewhat smaller than that from the Fermi three-parameter fit.

### DISCUSSION

If we consider only the Fermi fits, there is a reasonable consistency between the parameters found in the fits for the two energies. The  $\chi^2$  for the 400-MeV data is a bit large. However, one point ( $70^\circ$ ) contributes 5 to the total  $\chi^2$  value of 15. Because the 250-MeV data are less sensitive to  $w$ , the value of  $w$  found at 400 MeV is more reliable. The calculated rms radii are effectively the same. A change in  $w$  is compensated for by a change in  $c$ , but the radius remains the same. The shell-model fits have a larger  $\chi^2$  than the Fermi fit, and give disparate results between the two energies. However, the shell-model minimum is less deep than the Fermi fit. It appears that the shell-model charge distribution with the parameters  $a$  and  $\alpha$ , as indicated, do not describe the data away from the minima as well as the Fermi fits. It must be recalled that the data points in and near the diffraction minima were not included in any of the fits.

We are uncertain why there is such a poor fit at the diffraction minimum compared with neighboring nuclei. Neighboring nuclei (except  $N^{14}$ , in which a large quadrupole moment must be taken into account) are well fitted using the phase-shift technique and the Fermi distribution. On the other hand, there is no *a priori*

reason that the Fermi shape should fit all the nuclei. The energy and angular resolution of the experiment cannot account for the filled minimum. One conclusion is that there must be an additional contribution to the scattering, which is relatively important at the diffraction dip. In addition to pure charge scattering, one must consider the magnetic scattering from the magnetic moment, or a quadrupole moment contribution. But  $N^{15}$  has  $J=\frac{1}{2}$ ; therefore, it has no quadrupole moment. However, there could be a distortion of the nuclear shape that would contribute effects similar to a quadrupole moment. The magnetic moment of  $N^{15}$  is small (about a factor of 10 smaller than other  $p$ -shell nuclei), and estimates based on shell-model calculations yield a contribution to the cross section that is a factor of 50 or more too small to account for the filling in of the diffraction dip.<sup>13</sup> An appreciable amount of contaminant material of low atomic weight could cause the diffraction minimum to be filled in. Such a light nucleus would not be seen in the spectrum since it would not be kinematically separable. However, the analysis of the target material with the mass spectrometer shows no such contaminants. Another possibility is that there is an unknown, unresolved level in  $N^{15}$  whose relative contribution to the scattering cross section is sufficient in the region of the diffraction minimum to cause the observed effects. But results from low-energy nuclear spectroscopy show no such level. Dispersion effects are not expected to make a sufficient contribution to account for the discrepancy. Any of these effects would alter the values of the parameters that have been found for  $N^{15}$ . The amount of change of these parameters would be dependent on the nature and magnitude of any such contribution.

### ACKNOWLEDGMENTS

We would like to thank the many people who have assisted us in the several phases of this work. One of us (E. D.) would like to thank Professor Gorodetzky of the Institute de Recherches Nucleaires, Strasbourg, France, for his support during a visit there in the initial part of this work, and another (M. C.) wishes to express his gratitude to Professor Robert Hofstadter for his kind support during his stay at Stanford University. We wish also to thank Professor Hofstadter for placing the facilities of the Hansen Laboratory at our disposal for the experiment. Dr. Jochen H. Heisenberg has generously given us the use of his phase-shift program for the data analysis.

<sup>13</sup> See, e.g., R. E. Rand, R. Frosch, and M. R. Yearain, Phys. Rev. **144**, 859, (1966).